Sediment transport in the saltation regime

F. Osanloo,[1] M. R. Kolahchi,[1] S. McNamara,[2] and H. J. Herrmann[3]
[1]*Institute for Advanced Studies in Basic Sciences, P. O. Box 45195-1159, Zanjan, Iran*
[2]*Institute for Computer Physics, Stuttgart University, 70569 Stuttgart, Germany*
[3]*Computational Physics, IfB, ETH Zürich, Hönggerberg, 8093 Zürich, Switzerland*
(Received 21 May 2007; revised manuscript received 22 April 2008; published 3 July 2008)

We present a study of sediment transport in the creeping and saltation regimes. In our model, a bed of particles is simulated with the conventional event-driven method. The particles are considered as hard disks in a two-dimensional domain with periodic boundary conditions in the horizontal direction. The flow of the fluid over this bed of particles is modeled by imposing a force on each particle that depends on the velocity of the fluid at its height above the bed. We consider two velocity profiles for the fluid, parabolic and logarithmic. The first one models laminar flow and the second corresponds to turbulent flow. For each case we investigate the behavior of the saturated flux. We find that for the logarithmic profile, the saturated flux shows a quadratic increase with the strength of the flow, and for parabolic profile, a cubic increase. The velocity distribution functions are used to interpret the results.

DOI: 10.1103/PhysRevE.78.011301 PACS number(s): 45.70.Mg, 47.15.G−, 47.57.Gc

I. INTRODUCTION

The study of the transport of granular material by a fluid is important for industrial processes as well as for the understanding of natural phenomena. Modeling of the sediment transport in rivers, as well as modeling of sand drift in the formation of dunes, will benefit from this study.

Saltation, surface creep, and suspension are three modes which occur during transportation of granular material by a fluid [1]. When the shear velocity of the fluid flowing over a bed of grains exceeds the friction threshold velocity for sand transport, the grains are driven by the fluid. At first they begin to move while remaining in continual contact with each other, yet it could happen that every now and then due to collisions, some particles jump by a distance of order of their diameter. This regime is called surface creep or reptation. As the fluid shear velocity increases, the particles can follow paths that take them to a height much larger than their diameter; this regime is called saltation. The grains in saltation have been named saltons, and the grains in creeping motion have been named reptons [2]. Sediment transport as bed load usually moves in one of these two ways. Suspension occurs at very high shear velocities, when a considerable fraction of the particles are transported upwards by turbulent eddies. In this regime, the grains move in the fluid for long periods of time, hardly colliding with the bed or each other. Except for dust storms in which suspension is dominant, creeping and saltation usually play the key role in dune formation [3]. In many of the experimental studies of sediment transport, grains are transported by air [1,3,4], but a few experiments in water also exist [5,6].

Improvement in the modeling of sediment transport under the influence of a shear flow requires knowing the details of the grain trajectories. A few attempts have been made to derive a set of theoretical equations describing the trajectories of saltating grains. Each model has made some simplifications in solving the equations. Some authors [1,7] assume that the initial velocity of a saltating particle is vertical and proportional in magnitude to the shear velocity; this assumption is proper for high shear velocity. Ungar and Haff [8] suppose that for a given impact velocity a certain number of particles are ejected from the surface, all having the same ejection velocity. This velocity is constant and independent of shear velocity. In other theoretical work Wiberg and Smith [9] combine the equations of motion for a grain and those for the local fluid flow. This gives a set of equations that can be solved numerically to derive the trajectory of the grain with time. This model uses a minimal set of empirical constants and gives good agreement with the measured trajectory. Their model also derives the initial ejection velocity. However, this model is restricted to the motion of a single grain over a fixed bed. The authors [9] approximate bed load transport by averaging over saltating grains which move on a fixed rough bed. Thus it does not include the effect of collisions between moving particles. To avoid these restrictions Jiang and Haff [10] present a model to follow the trajectories of each of the moving particles over a two-dimensional bed. The fluid is modeled as a moving layer or slab which exerts a velocity dependent drag force on the embedded grains. However, the slab model does not consider the detailed vertical velocity structure and just the upper particles experience the effect of the slab.

In the present study we investigate sediment transport for the case that a fluid with a certain velocity profile flows over a bed initially at rest. The motion of the particles is caused by aerodynamic entrainment or collisions with other particles. We do not apply any restriction to the initial velocity of the grains. The bed is not fixed and we can follow the trajectory of the grains with time; their collisions with each other and with the moving bed are also included.

To gain insight into the problem of the sediment transport, it is important to understand the relation between the flux of the grains, bed-load transport rate, and the velocity profile of the fluid. An application of the study of sand flux is in geomorphology where it becomes necessary to calculate the erosion rate in order to predict the evolution of a free sand surface or a dune. In most instances of sediment transport, the flux eventually saturates at a certain strength or amplitude u_* of the velocity profile $v(y)=u_* f(y)$. Here, f is a func-

tion of height y. There has been a great effort to obtain experimentally [1,4,11], and theoretically [1,7,8,12,13] the relationship between the saturated granular flux over a bed and the shear velocity. Bagnold [1] was first to introduce a simple flux law, a cubic relation, expressing the dependence of sand flux on the shear velocity. Apart from the work by Ungar and Haff all the above theoretical studies give similar results; the saturated flux q scales at large shear velocity similar to the Bagnold description and vanishes below a threshold value. The model given by Ungar and Haff predicts that the flux increase is slower than u_*^3. Almeida *et al.* [14] also obtain numerically a quadratic relation near the threshold shear velocity. Most of these studies analyze only the longitudinal, down-stream component of particle displacement, and neglect any lateral movement. Lateral motion of grains will be important in studying the grain trajectory in the intermediate range and in studying the diffusion of saltating particles [15]. Although much work has been devoted to the sediment transport, the problem of predicting the bed-load transport, that is the main practical quantity of interest, is as yet not satisfactorily studied for either of turbulent or laminar flows.

The goal of our paper is to find the dependence of the flux on shear velocity u_* for a system that has a transition from creep to saltation. We consider two velocity profiles for the fluid, logarithmic and parabolic. Although there are studies for the logarithmic profile, we do not know of similar studies for the parabolic profile. In fact, most of the existing data are for turbulent flows, but some experiments on dynamics of a bed of particles sheared by laminar flow also exist [16]. We did not restrict ourselves to only saltation as most of the previous models; nor only to creep. The only model that considers two types of particles in transport, saltons and reptons, has been proposed by Andreotti [17] in which the dynamical mechanisms governing the saturation of the sand flux were investigated.

We emphasize that for the purposes of this study, saltation has a different meaning than its standard usage. For instance, in a wind tunnel, a grain is in saltation if its trajectory is at least about 300 grain diameters high and at least 1000 grain diameters across. These are much larger than the size of the system considered here. Yet, we use this term to distinguish the motion from the situation where the grains constantly touch each other as they move. Saltation is then used to mean a motion where the grains jump and follow a trajectory, albeit smaller than mentioned above.

The structure of the paper is as follows. In Sec. II we introduce the model. Then in Sec. III, we study the behavior of the flux as a function of the velocity profile, as well as the velocity distribution functions for the grains and compare the velocity distributions for the two profiles. Finally, we present our conclusions as Sec. IV.

II. SIMULATION MODEL

We use the inelastic hard sphere model [18]. Grains are contained in a two-dimensional rectangular domain with periodic boundary conditions in the horizontal directions. The fluid flows over the bed of grains, so grains can be entrained by the fluid. The fluid is modeled by its velocity profile.

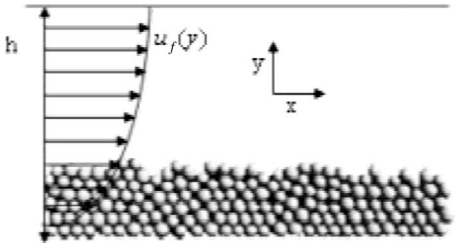

FIG. 1. The schematic representation of the system showing the particles in their initial state, and the velocity field at different places along the y axis.

The grains, modeled as disks, move under the influence of both gravity and a drag force that is exerted on them by the fluid. To avoid crystallizations, 20% of the particles have a diameter equal to $0.6l_0$ and the rest have a diameter equal to $0.5l_0$, where l_0 is the unit of length used throughout this paper [19]. Although this implies that particles would have different mass, we suppose that particles have the same mass. We make this choice because this difference in size is not intended to model different particle sizes, but merely to prevent crystallization. A gravitational acceleration of $12l_0/t_0^2$ is applied to all the particles, where t_0 is the unit of time.

In all cases studied, the system starts out having six layers of particles resting fairly compactly on each other. The fluid stands at a height that is equivalent to thirty two layers $16l_0$. This height is the maximum attainable by the grains; because in our modelization we implement a reflecting boundary at the top so that the particles that touch it just reverse their vertical velocity component. The system is sketched in Fig. 1.

A. Particle motion

We use event-driven MD [20] to calculate the motion of the particles. As the particles are hard spheres, collisions take infinitesimal time and involve only two particles. Conservation of momentum for two spherical particles with masses m_1 and m_2 leads to

$$\vec{u}_{1,2} = \vec{v}_{1,2} \mp (1+r)\frac{m_{2,1}}{m_1+m_2}[\hat{K}\cdot(\vec{v}_1-\vec{v}_2)] \times \hat{K} \mp \frac{2}{7}(1+\beta)\frac{m_{2,1}}{m_1+m_2}[\hat{t}\cdot(\vec{v}_1-\vec{v}_2)]\hat{t}, \quad (1)$$

where $\vec{u}$ indicates the velocities after the collision and $\vec{v}$ denotes the velocities before the collision. The geometry of the collision is described by $\hat{K}$, a unit vector pointing from the center of particle 1 toward the center of particle 2, and $\hat{t}$ is the unit vector in tangential direction. The energy dissipation is controlled by r, the normal restitution coefficient, and β, the tangential restitution coefficient. If $r=1$ and $\beta=\pm 1$, collisions conserve energy and are said to be elastic. For $0<r<1$ or $-1<\beta<1$ energy is dissipated and the collisions are inelastic. In our simulations, $r=0.4$ and $\beta=-1$.

We assume that the particles neither rotate nor roll on each other. This is in accord with the fact that the sand grains

are not round so that rolling is difficult. For saltons the mean waiting time, that is the time between two consecutive collisions, is about $0.02t_0$ (the mean velocity of the saltating grains is about 15 so that during this time a particle in saltation would travel $0.3l_0$ compared to $0.5l_0$ which is the diameter of the grain). As the particles are small the vertical gradient of force across the diameter of the particles is small and creates a small torque on particles. The rotation of a particle under this torque during the time mentioned is negligible. The ratio of the kinetic energy of rotation to the kinetic energy of translation of the grains is about 0.001. The reptons that just move over the bed, have very small energy. They cannot eject other particles from the bed so they cannot affect the granular bed whether they rotate or not. So we can neglect their rotation.

In using the event-driven method there are two problems in setting up the bed of grains: inelastic collapse and creating a rough surface on the bottom. All particles after some collisions lose their energy and accumulate on the bottom and make a dense network of grains. So the number of collisions per unit time will diverge at finite time; that is, inelastic collapse [21] will occur. Because of the finite precision of the computer, multiparticle collisions can occur. For handling the inelastic collapse we use the T_c model with $t_c=10^{-6}t_0$ [21].

In order to create a rough surface, r and β are adjusted for collisions between the grains and the surface. We suppose that when a particle of the bottom layer bounces against the bottom plate both the tangential and normal components of its velocity are reversed, i.e., $r=1$ and $\beta=1$ in Eq. (1). In this way, the first layer is nearly fixed and acts as a rough surface over which other particles can move. The roughness is of the order of the particle diameter.

B. Effect of fluid on the grains

The drag force is proportional to the difference between the particle velocity $\vec{u}_p$ and the fluid velocity $\vec{u}_f$:

$$\vec{F}=\gamma(\vec{u}_f-\vec{u}_p), \tag{2}$$

where γ is a parameter that depends on the characteristics of both the fluid and the grains. In laminar flow with small Reynolds number $\gamma=3\pi\eta d_p$, in which η is the viscosity of the fluid and d_p is the diameter of the particle. We suppose that $\gamma=1$ for laminar flow. However in turbulent flow, the fluid drag varies as the square of the grain speed and γ can be written as

$$\gamma=\frac{3C_D\rho_f}{4\rho_p d_p}|\vec{u}_f-\vec{u}_p|, \tag{3}$$

which corresponds to the Newtonian drag force per unit particle mass where C_D is taken from empirical relations and ρ_f and ρ_p are the density of the fluid and particle, respectively.

In general, the drag force acts on upper layers of the bed of particles and drops to zero for lower layers. The details depend on the velocity profile considered. Here, we study the dynamics of the grains for two velocity profiles: logarithmic and parabolic. The parabolic profile models laminar flow in inclined open channels driven by gravity and without a streamwise pressure gradient. In this case, the fluid velocity is

$$u_f=u_*[y_0(y_0/2-h)-y(y/2-h)], \tag{4}$$

where h is the height of fluid in channel. This equation is written so that it satisfies the two boundary conditions $\partial u_f/\partial y=0$ at $y=h$ and $u_f=0$ at $y=y_0$. Here, y is the vertical coordinate and $y_0=0.5l_0$ is the height below which the effect of the fluid on the grains is negligible. Indeed, The first term of the Eq. (4) is an offset which means that the zero of the profile is inside of the granular bed. This is so because there is also a certain flow of fluid through the packing beneath the surface. The slope of the channel is very small, just enough to drive the flow.

In turbulent flow, the velocity profile of the fluid near the boundary is observed to be logarithmic [22], and described by

$$u_f=\frac{u_*}{k}\ln(y/y_0), \tag{5}$$

where k is the von Karman constant and u_* is the shear velocity that is defined as $u_*=(\tau_b/\rho)^{1/2}$, where τ_b and ρ are the bottom shear stress and fluid density, respectively. Although this relationship has been derived only for the region where the shear stress is approximately constant, experiments show that the agreement persists through almost all of the boundary layer. In our simulations $y_0=0.5l_0$. We consider no vertical component to the fluid velocity. The vertical component of fluid velocity is small compared to the mean forward velocity over the ground at low height. It may be important in the study of the suspension regime.

For the purposes of the present study it is reasonable to neglect the effect of particles on the fluid, since in our system most of the particles stay on the ground or are close to it. At the same time the saltation is very low and weak, so we can include the feedback in our shift of the zero of the profile (which we discussed above). An estimate which again points to the same conclusion is provided by the ratio of the momentum flux of the grains to that of the fluid. In steady state we find this to vary from 3% at the smallest u_* in our study to about 20% at the highest u_* studied. This implies that in studying the creep regime as well as the onset of saltation, neglecting the feedback is a reasonable approximation.

III. GRANULAR FLUX AND VELOCITY PROBABILITY DISTRIBUTION FUNCTION

First we investigate the behavior of the granular flux with respect to time. Granular flux is the total amount of material transported by the flow, or the average number of particles per unit time that cross a surface perpendicular to the flow. In two dimensions, one can simply determine the rate at which particles cross a vertical line. If this quantity is averaged over the entire domain, one obtains

$$q=\frac{1}{L}\sum_{i=1}^{N}u_i, \tag{6}$$

where L is the length of the box and N is the total number of particles.

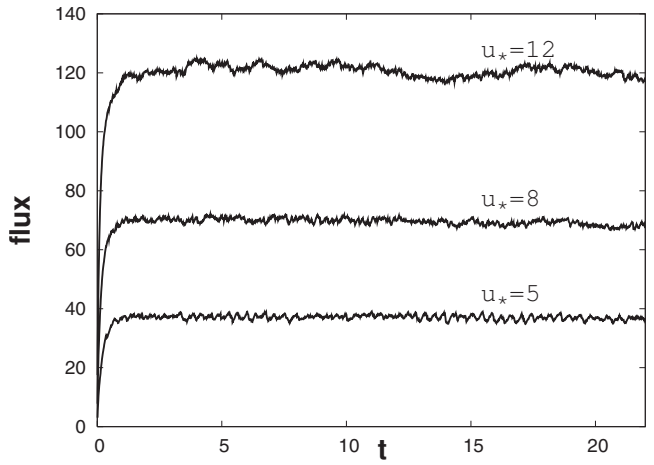

FIG. 2. Flux as a function of time for different values of u_* for a logarithmic profile.

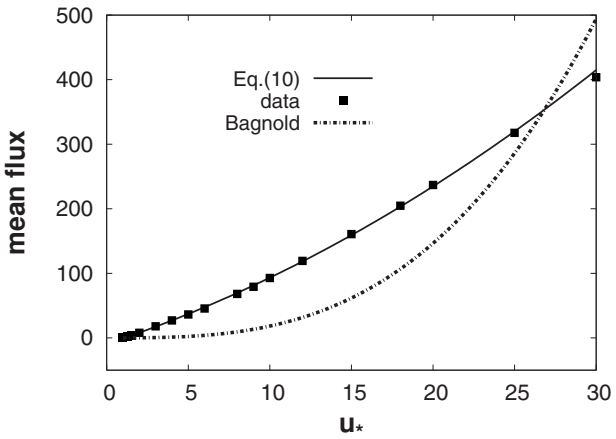

FIG. 3. Mean flux vs u_* for a logarithmic profile: Eq. (10) compared to Bagnold's expression. Fit to Eq. (10) gives $a=0.2$, $b=43.9$, and $u_t=1.09$. According to the simulations we set $u_t=1$, as an estimate.

After some time the flux fluctuates around a constant, steady value, and sediment transport reaches steady state. This steady state is the saturated flux, and it depends on the shear velocity, denoted by u_*.

For calculating the saturated flux value, we average over the flux only after the steady state has been reached. We expect to have a threshold velocity u_t, below which sediment transport cannot happen.

In order to determine the evolution of the particle velocity we study the velocity probability distribution function (PDF). The range of velocities is divided into intervals of width 0.2. When the system reaches steady state, we count the particles whose velocity lies within each interval; this makes up the PDF at that time. Then we repeat this for 2500 times at intervals of $0.01t_0$, and finally we arrive at the steady state PDF by averaging over the 2500 PDFs found.

A. Logarithmic profile

In the Aeolian case, the logarithmic velocity profile is more realistic than the parabolic profile. When the wind blows over a rough surface, its velocity within the boundary layer increases logarithmically with height as in Eq. (5). The logarithmic profile has also been observed experimentally, for water moving over a rough surface in a channel [5,6].

Figure 2 shows the variation of flux with time for different values of shear velocity u_*. This figure shows that flux reaches steady state and saturates after some transient.

The simulations could be made into movies of the grain motion. This was a particularly useful way of interpreting the results. In this way we estimate that grain motion starts at a threshold velocity of about $u_*=u_t=1$. As u_* increases above the threshold, the top layer particles begin to roll in their own layer or jump to a height about their diameter. This situation continues until $u_*\simeq 15$. This means that for $u_*<15$ most of the particles except those in the bottom layer are in the creeping regime. After $u_*>15$ the shear stress is enough to make some of the particles in the upper layers enter the saltation regime. With increasing u_*, the number of saltating particles increases, resulting in an increase in the number of collisions between saltons. We estimate $u_*\simeq 15$ as marking the onset of saltation in this system. When $u_*>30$ enough particles have so high an energy that they move with the fluid stream above the other particles and have few collisions with each other or the rest of the grains. In this case the length of their trajectory becomes comparable to the system size, hence we only considered $u_*<30$. We wish to emphasize again that we are using the term saltation in a restricted sense in this study.

The main objective of this study is to relate the saturated flux and the shear velocity in the regime of saltation. In Fig. 3 we show the mean particle flux as a function of u_*.

Theoretically, perhaps the most important description for saturated flux is due to Bagnold [1]. He found that the saturated flux at large shear velocities is given by

$$q=\frac{\rho_{\text{air}}}{g}u_*^3. \tag{7}$$

Bagnold considered a mean trajectory for each grain, and supposed that the ejection velocity of grains from the bed scales with the shear velocity u_*. This hypothesis is valid if the shear velocity is large enough. For small shear velocities, Ungar and Haff [8] supposed that height and length of the trajectory of grains is of the same order as the grain size, and predicted that

$$q\propto\rho_{\text{air}}(u_*^2-u_t^2)\sqrt{\frac{d}{g}}, \tag{8}$$

where d is the grain diameter. In their numerical study Almeida et *al.* [14] also found numerically a quadratic description for the flux near the threshold shear velocity

$$q\propto(u_*-u_t)^2. \tag{9}$$

They simulated the saltation inside a two-dimensional channel with a mobile top wall. Their model solves the turbulent wind field including the feedback from the dragged particles.

Our results show a slightly different quadratic dependence

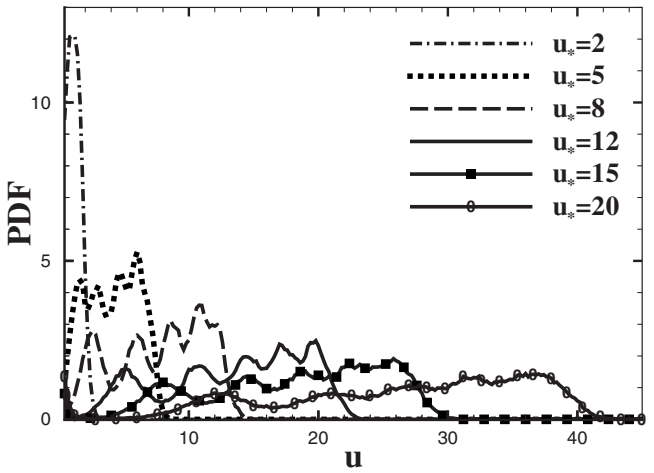

FIG. 4. The grain longitudinal velocity probability distribution function for different values of u_* for the logarithmic profile.

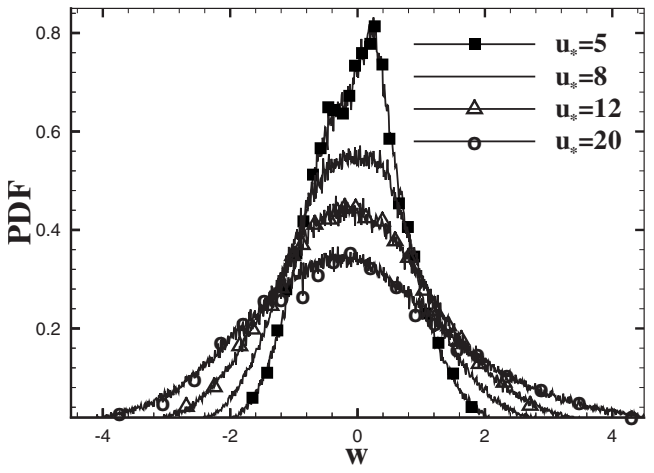

FIG. 5. The grain transverse velocity probability distribution function for different values of u_* for the logarithmic profile.

$$q = a(u_* - u_t)(u_* + b), \tag{10}$$

where $a=0.2$, $b=43.9$, and $u_t=1.09$ are obtained from fitting Eq. (10) to our data. This value for the threshold velocity is in good agreement with the estimate from the simulations; that is $u_t=1$. Figure 3 shows the fit of Eq. (10) to the data. This indicates that the same quadratic function describes the behavior of flux reasonably well in both the creeping and saltating regimes. Equation (10) predicts a stronger dependence on shear velocity than Eq. (9). One reason may be our neglect of the feedback of the grains on the fluid. This effect is more prominent at small heights where the particle velocity differs much from the fluid velocity [14].

Another way to estimate the onset of saltation is to investigate the grain longitudinal velocity (u) probability distribution function. The distribution function allows decomposition of the flux into a part due to saltation and another part due to creep. This interpretation is based on the fact that the reptons are slower than the saltons. Figure 4 shows the behavior of the grain longitudinal velocity distribution for different values of u_*.

For small values of u_* there is a large peak at small velocities that shows that all of the particles are in creeping motion. With increasing u_*, the velocity of the particles increases and some of the particles enter the saltation regime. The uniform distribution function at higher velocities represents the saltons. For example, at $u_*=15$ many particles are saltons; the velocity distribution develops a minimum at $u \sim 2$. At $u_* \sim 20$ all of particles are saltating.

The distribution of the transverse (vertical) velocity w of the grains is also investigated. The PDF of w is shown in Fig. 5 for different u_*. When most of the particles are saltating it is close to a Gaussian with zero mean. At the onset of creep, it deviates from a Gaussian because most of the particles are at rest. At higher shear velocities, the transverse velocities fluctuate around zero because of collisions between moving particles. As we will see in the next section, the PDF of the transverse velocity for parabolic profile of the fluid is also a Gaussian. There is small drag due to vertical motion of particles with respect to the fluid, similar to the transverse (radial) motion of particles in Charru *et al.* [16]. Charru *et al.* also observe a Gaussian PDF in the transverse direction.

The Gaussian distribution implies that the system acts as if it were in equilibrium in the transverse direction. So, a granular temperature proportional to $\langle w^2 \rangle$ for random motion in transverse direction can be defined. As Fig. 5 shows, this temperature increases with u_*.

B. Parabolic profile

At low Reynolds numbers when a fluid flows in a sloping open channel, its velocity varies with height parabolically. Now, we consider a velocity profile as in Eq. (4), that is zero at the bottom and increases parabolically with height.

Figure 6 shows the behavior of flux as a function of time. Similar to the logarithmic profile, the flux reaches steady state, only now the transient time is longer. In the parabolic profile, the shear stress above the bed is greater than the logarithmic profile and increases rapidly with u_*, so compared to the logarithmic case, the range of u_* that defines the creep motion is much narrower.

The motion starts out at about $u_t=0.08$ [23]; this is an estimate obtained from our simulations. When $u_*=1$ the sys-

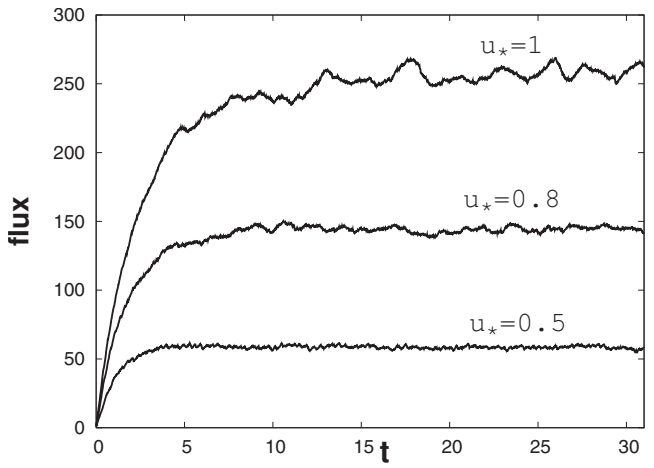

FIG. 6. Flux as a function of time for a parabolic profile.

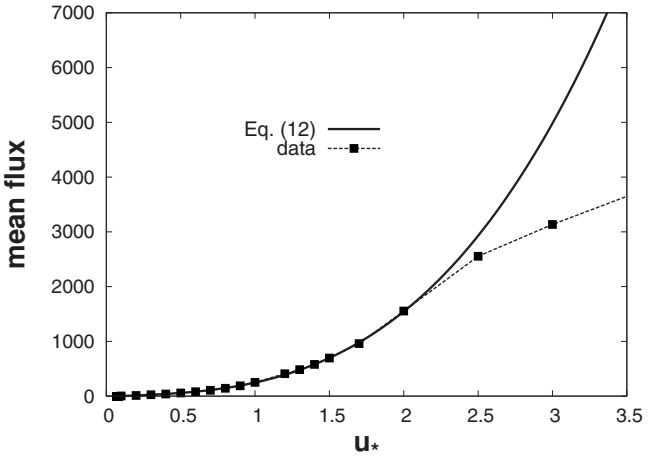

FIG. 7. Mean flux as a function of u_* for a parabolic profile. The dashed line is our data, and the solid line is a fitted cubic polynomial to data. Beyond $u_* \sim 2.5$ the effect of the "top boundary" is revealed. $u_t = 0.08$ is estimated from the simulations.

tem is out of the creeping regime, and starts saltating. The surface $y=h$ is as before a reflecting surface, so any particle that reaches it bounces back into the fluid. This starts at about $u_*=1.2$. Beyond $u_*=1.5$, all particles are in the saltation regime. In Fig. 7 we show the mean flux vs u_*. As observed beyond $u_*=2.5$ this boundary produces a kind of population inversion and the collision of particles with each other effectively reduces the rate of increase of flux.

In Fig. 8 we show the behavior of the mean flux with u_* (near u_t). For $u_*<1$ we fitted the data with two equations below:

$$q = a'(u_* - b')^2, \tag{11}$$

$$q = a(u_* - 0.08)(u_*^2 + bu_* + c). \tag{12}$$

The values of $a'=258$, $a=182$, $b=-0.07$, $c=0.5$, and $b'=0.036$ are obtained from fitting. In Eq. (12), $u_t=0.08$ is used

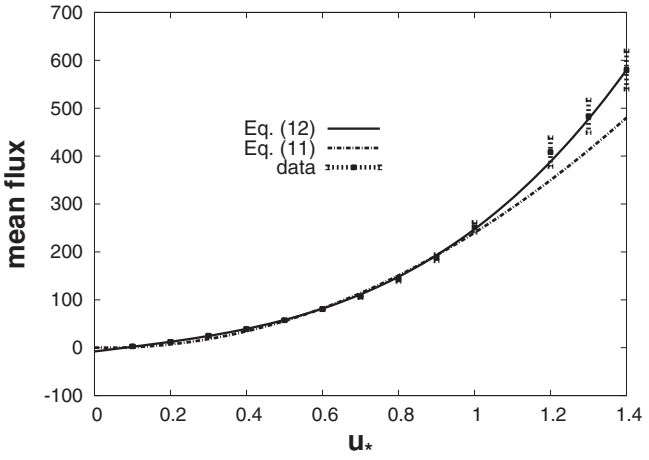

FIG. 8. Mean flux as a function of u_* near the threshold value $u_t=0.08$ for a parabolic profile. For $u_*<1$ we fitted the data with two Eqs. (11) and (12). The solid line is the fit using Eq. (12) yielding $a=182$, $b=-0.07$, and $c=0.5$. The dashed line is the fit using Eq. (11) that gives $a'=258$, and $b'=0.036$.

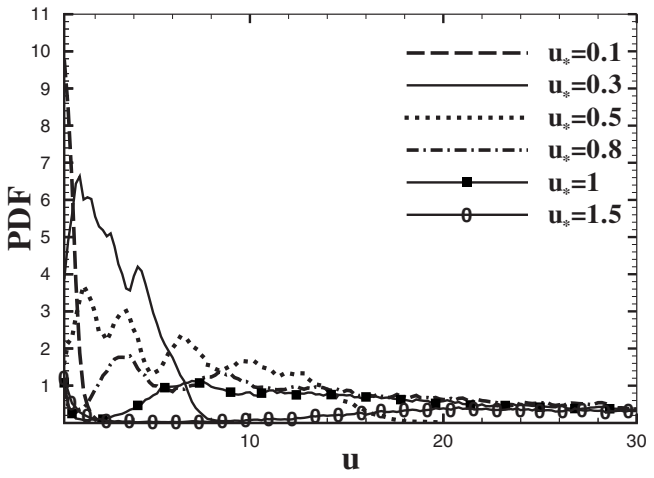

FIG. 9. The grain longitudinal velocity probability distribution function for different values of u_* for a parabolic profile.

as an input data. The cubic equation is clearly a better fit to the data than the quadratic one.

Let us compare the logarithmic and parabolic profiles using the grain velocity distribution functions. With increasing shear we expect to have more and more particles in motion. The probability distribution function of longitudinal velocity, develops a peak at low velocities $u \sim 2$ that gradually disappears as u_* increases. In case of the logarithmic profile, Fig. 4, this peak does not broaden. With the diminishing of this low-energy peak, a plateau is developed in the velocity distribution. This plateau which gradually covers a larger range of velocities, corresponds to saltons. The density of particles in the saltation regime, for the logarithmic profile, is a monotonically decreasing function of height. We attribute this to the small energy input rate; which goes as $q_f u_f^2$, where q_f is the fluid flux.

For the parabolic profile, Fig. 9, the situation is markedly different. We observe that as the shear velocity increases, the distribution develops a tail, covering the larger velocities. The rate of energy input is much higher in the case of the parabolic profile. In the saltation regime ($u_* \geq 0.8$), it is possible to distinguish a group of particles moving at a higher velocity and height, nearly separated from the rest of the particles. In this sense, the density of particles in the saltation regime, is very different from that of the logarithmic velocity profile. This explains the sudden velocity spread at $u_* \geq 0.8$.

Figure 10 shows the transverse PDF for the parabolic profile. Similar to the logarithmic profile, once in the saltation regime the transverse PDF is nearly Gaussian with nearly zero mean. With increasing u_* the Gaussian becomes broader implying an increase in the granular temperature.

IV. CONCLUSION

In this study, we have presented a simple model for creeping and saltating motion that produces steady sediment transport. We investigated the steady state flux for the parabolic and logarithmic fluid velocity profiles.

For the logarithmic profile we compared our results with previous similar studies. Increasing the shear velocity u_*

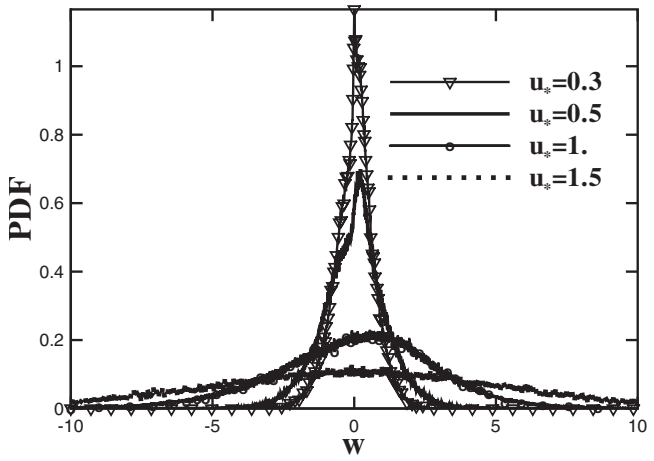

FIG. 10. The grain transverse velocity probability distribution function for different values of u_* for a parabolic profile.

from the threshold value u_t, sediment transport sets in, first creeping and then for larger u_*, saltating. In our system, the saltating particles can rise up to several times their diameter, and similar to Ungar and Haff [8] we find that the steady state flux increases quadratically with shear velocity. The fact that we recover asymptotically the quadratic relation of Ungar and Haff is reasonable. Since we did not explicitly incorporate the shear going as u_*^2 in our simulation, this can be regarded as a consistency check. In addition, our result Eq. (10) is not exactly as Eq. (8) of Ungar and Haff, and this can be attributed to their simplifying assumptions about how the particles impart momentum to the surface.

For the parabolic profile, that models a laminar flow, the flux rises cubically with increasing shear velocity. We also find that near the threshold velocity a quadratic expression fits our data as well as a cubic expression. Typical applications of our study of the sediment transport by a laminar flow are in hydraulic engineering. They are also important in the understanding of ripples and dunes or other pattern formations; as for example, when studying the pattern formations in the experiments conducted by Daerr *et al.* [24]. They have designed the experiment on a laboratory scale to reproduce a rich variety of natural patterns, especially intriguing rhomboid structures often found on sandy shores. The patterns are created by a falling water level on an erodible sediment layer that occurs naturally when the sea retreats from the shore.

The present study of discrete particles of bed-load sediment transport also helps us predict the creation and evolution of pattern formations in binary granular mixtures of sand bed. Also the process of segregation by size and density and its effects on pattern formation can be explored. The study of the details of the transport mechanism by turbulent and laminar flow might help us understand the pattern formation not only on Earth but also other planets such as Mars.

The velocity probability distribution function is a good measure to estimate the onset of saltation. It would be interesting to study a system large enough so that the grain velocity distribution function can be measured as a function of height.

ACKNOWLEDGMENTS

Part of this work was carried out while F. Osanloo stayed at the University of Stuttgart. She wishes to thank the University of Stuttgart for their hospitality and the grant that made her stay possible.

[1] R. A. Bagnold, *The Physics of Blown Sand and Desert Dunes* (Chapman and Hall, London, 1941).
[2] B. Andreotti, P. Claudin, and S. Douady, Eur. Phys. J. B **28**, 321 (2002).
[3] Y.-H. Zhou, X. Guo, and X. J. Zheng, Phys. Rev. E **66**, 021305 (2002).
[4] K. Nishimura and J. C. R. Hunt, J. Fluid Mech. **417**, 77 (2000).
[5] C. Ancey, F. Bigillon, P. Frey, J. Lanier, and R. Ducret, Phys. Rev. E **66**, 036306 (2002).
[6] C. Ancey, F. Bigillon, P. Frey, and R. Ducret, Phys. Rev. E **67**, 011303 (2003).
[7] P. R. Owen, J. Fluid Mech. **20**, 225 (1964).
[8] J. E. Ungar and P. K. Haff, Sedimentology **34**, 289 (1987).
[9] P. L. Wiberg and J. D. Smith, J. Geophys. Res. **90**, 7341 (1985).
[10] Z. Jiang and P. K. Haff, Water Resour. Res. **29**, 399 (1993).
[11] K. Lettau and H. Lettau, in *Exploring the World's Driest Climate*, edited by H. Lettau and K. Lettau (Center for Climate Research, University of Wisconsin, Madison, 1978).
[12] G. Sauermann, K. Kroy, and H. J. Herrmann, Phys. Rev. E **64**, 031305 (2001).
[13] M. Sorensen, Acta Mech. **1**, 67 (1991).
[14] M. P. Almeida, J. S. Andrade, Jr., and H. J. Herrmann, Phys. Rev. Lett. **96**, 018001 (2006).
[15] V. Nikora, J. Heald, D. Goring, and I. McEwan, J. Phys. A **34**, L743 (2001).
[16] F. Charru, H. Mouilleron, and O. Eiff, J. Fluid Mech. **519**, 55 (2004).
[17] B. Andreotti, J. Fluid Mech. **510**, 47 (2004).
[18] S. McNamara and W. R. Young, Phys. Rev. E **53**, 5089 (1996).
[19] Throughout this paper the unit of length is $l_0=2\times10^{-1}$ cm, and the gravitational acceleration of $12l_0/t_0^2=490$ cm/s^2 is applied to all the particles. This is the acceleration experienced by a particle with density of 2 g/cm^3 in water. The corresponding unit of time is 7×10^{-2} s.
[20] B. D. Lubachevsky, J. Comput. Phys. **94**, 255 (1991).
[21] S. Luding and S. McNamara, Granular Matter **1**, 113 (1998).
[22] A. Vardy, *Fluid Principles* (McGraw-Hill, New York, 1990).
[23] Although the threshold velocities for the two profiles are drastically different, the resulting drag forces (for the top layer), using Eqs. (2)–(5), come out nearly the same for both profiles, as expected, at the onset of motion.
[24] A. Daerr, P. Lee, J. Lanuza, and E. Clément, Phys. Rev. E **67**, 065201(R) (2003).